Depinning of a vortex chain in a disordered flow channel

R. Besseling[1], T. Dröse[2], V.M. Vinokur[3] and P.H. Kes[1]
[1] *Kamerlingh Onnes Laboratorium, Leiden University, P.O. Box 9504, 2300 RA Leiden, the Netherlands.*
[2] *I. Institut für Theoretische Physik, Universität Hamburg, Jungiusstrasse 9, D-20355 Hamburg, Germany.*
[3] *Materials Science Division, Argonne National Laboratory, Argonne, Illinois 60439*
(February 1, 2008)

We study depinning of vortex chains in channels formed by static, disordered vortex arrays. Depinning is governed either by the barrier for defect nucleation or for defect motion, depending on whether the chain periodicity is commensurate or incommensurate with the surrounding arrays. We analyze the reduction of the gap between these barriers as function of disorder. At large disorder, commensurability becomes irrelevant and the pinning force is reduced to a small fraction of the ideal shear strength of ordered channels. Implications for experiments on channel devices are discussed.

74.25.Qt; 71.45.Lr; 83.50.Lh

The depinning and dynamics of periodic elastic media in a random potential have received a great deal of recent attention [1]. It was shown, in particular for vortex lattices (VL's) in superconductors, that the depinning transition in most cases involves plastic deformations [2]. A system in which plastic depinning can be studied in a controlled way is that of narrow, weak pinning flow channels in a superconducting film [3]. In such a system, strongly pinned vortices in the channel edges (CE's) provide confinement as well as an effective pinning potential for chains of vortices inside the channel. By changing the magnetic field B, one can vary the ratio between channel width and lattice spacing and thus induce incommensurability between the vortex spacing inside and outside the channel. This leads to topological defects in the channel which sensitively affect the threshold for plastic flow, as evidenced by oscillations of the critical current density J_c versus field [3].

Simulations of channels with perfect *hexagonal* vortex arrays in the CE's, showed sharp peaks in J_c for channel widths w equal to an integer number n of vortex row spacings, i.e. $w = nb_0$. At mismatch ($w \neq b_0$) defects occurred in the channel and J_c vanished due to the small Peierls barrier for defect flow [4]. This however contrasts the smooth oscillations found experimentally. Moreover, in reality the CE arrays may contain *quenched positional disorder* due to random pinning. This should modify J_c and its dependence on commensurability. In this Letter we consider the most simple near-to-commensurability situation $w \sim b_0$, and investigate the effect of disorder on depinning of a *single vortex chain*. We find that commensurate chains, with a periodicity equal to that of the VL in the CE's, depin at a force f_n below the ideal shear strength f_c^0 by *nucleation of defect pairs*. At incommensurability, f_c is determined by the pinning force f_d of *existing defects*. At weak disorder, a gap is found between f_n and f_d, but for larger disorder commensurability becomes irrelevant and f_c saturates at a small fraction of f_c^0. This has important consequences for the interpretation of the experiments [3]. Generally, our results are relevant to a wealth of 1D problems including models for interface growth [5], dynamics of Josephson junctions [6] and charge density waves (CDW's).

We consider a channel at $T = 0$ with boundaries (CE's) formed by two *static*, disordered arrays with vortex positions $\mathbf{R}_{n,m} = \mathbf{r}_{n,m} + \mathbf{d}_{n,m}$, where $\mathbf{r}_{n,m}$ denote the hexagonal lattice with spacing $a_0 = 2b_0/\sqrt{3}$ (see the inset to Fig. 1), the channel width is defined by the spacing between rows $m = \pm 1$ and $\mathbf{d}_{n,m}$ are random shifts. We restrict ourselves to longitudinal shifts [7] and choose $\mathbf{d}_{n,m} = d_n \vec{e}_x$ such that the *strain* $(d_{n+1} - d_n)/a_0$ is uniformly distributed in the interval $[-\Delta, \Delta]$ with Δ the disorder parameter. The field B sets both the vortex density in the CE's ($\rho_e = (a_0 b_0)^{-1} = B/\Phi_0$ with Φ_0 the flux quantum) and the density $\rho_c = (aw)^{-1}$ *inside* the channel. Hence, vortices *in* the channel have an average spacing $a = a_0 b_0/w$ which can be commensurate with the CE arrays ($w = b_0$, $a = a_0$) or incommensurate ($a \neq a_0$). The equation of motion for vortex i in the channel is:

$$\gamma \partial_t \mathbf{r}_i = f - \sum_{j \neq i} \nabla V(\mathbf{r}_i - \mathbf{r}_j) - \sum_{n,m} \nabla V(\mathbf{r}_i - \mathbf{R}_{n,m}). \quad (1)$$

$V(\mathbf{r})$ is the interaction potential, j labels other vortices in the channel, $\gamma = B\Phi_0/\rho_f$ with ρ_f the flux flow resistivity and $f = J\Phi_0$ is the drive along x due to a uniform current density J applied perpendicular to the channel.

For $\Delta = 0$ the vortex chain can be described by a Frenkel-Kontorova model for interacting particles in a periodic potential [4]. The ratio between the chain stiffness and the height of the periodic potential is given by $g \propto \lambda/a_0 \gg 1$ with λ the penetration depth. A commensurate chain depins uniformly at a critical force $f_c = \mu = 2a_0 c_{66}/\pi\sqrt{3}$ (c_{66} is the shear modulus) with a velocity $v = \sqrt{f^2 - \mu^2}/\gamma$. At incommensurability, defects of size $l_d = 2\pi a_0 \sqrt{g} \gg a_0$ are generated. Their pinning barrier and the critical force are essentially vanishing. For $f < \mu$ and small defect density, given by $c_d = |a_0^{-1} - a^{-1}| \lesssim l_d^{-1}$, the motion of defects leads to a low mobility regime where

$v = c_d v_d^0 a_0$ with $v_d^0 = (\pi^2\sqrt{g}/2\gamma)f$ the pure defect velocity [8].

We start with a numerical study of the behavior in presence of disorder. Eq. (1) was solved using a modified London form for $V(\mathbf{r})$ which yields the correct shear modulus [4]. We used cyclic boundary conditions, channels of length $L \geq 1000a_0$ and we recorded the velocity $v(f) = \langle \dot{x}_i \rangle_{i,t}$ and vortex positions $x_i(t)$.

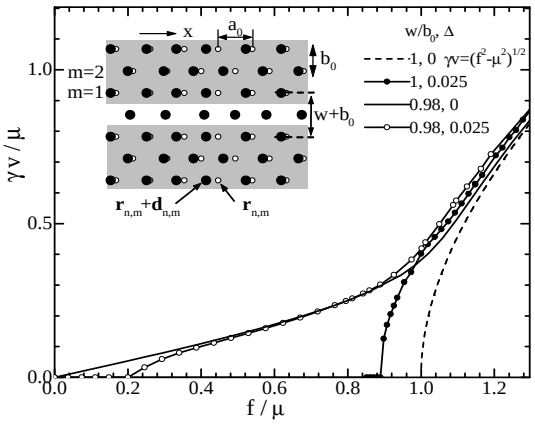

FIG. 1. Simulated *f-v* curves at weak disorder ($\Delta = 0.025$) for $w/b_0 = 1$ (•) and $w/b_0 = 0.98$ (◦) (dashed and full lines are the respective results for $\Delta = 0$). Inset: channel geometry with pinned vortices in the gray areas. Their equilibrium positions $\mathbf{r}_{n,m}$ are denoted by (◦). The disordered arrays (with the shifts d_x exaggerated for clarity) are denoted by (•).

The data points in Fig. 1 show *f-v* curves of a commensurate and an incommensurate chain for $\Delta = 0.025$. We first focus on the commensurate case. Compared to the result for ordered CE's (dashed line), f_c in presence of disorder is clearly reduced. The origin of this reduction is that the random strains lower the energy barrier for formation of discommensuration pairs in the chain (interstitial/vacancy pairs in the 2D crystal formed by the chain and the CE's).

We show the depinning process in detail in Fig. 2a by plotting the time evolution of the displacements $u_i = x_i - ia_0$ [9]. At $t = t_1$, the force is increased to a value $f > f_c$. The motion starts at an unstable site in the chain by nucleation of a vacancy/interstitial pair shown as steps of $\pm a_0$ in u. We denote the force at which this local nucleation occurs by f_n. The process at this site repeats periodically with rate $R_n \propto (f - f_n)^\beta$ and a depinning exponent $\beta = 0.46 \pm 0.04$, as previously reported for 1D periodic media [10]. Due to the nucleation center, a domain forms with defect density $c_d = R_n/\langle v_d \rangle$ and a net velocity $v = c_d \langle v_d \rangle a_0 = R_n a_0$ with $\langle v_d \rangle$ the average defect velocity $\simeq v_d^0$, see below. In a larger system (Fig. 2b), a distribution of unstable sites p with local rate $R_{n,p}$ initially leads to the growth of several domains. However, when two domains with rates $R_{n,1} > R_{n,2}$ meet, their interstitials and vacancies annihilate and domain 1, with the larger nucleation rate, then expands at the cost of domain 2 with a rate $\sim (R_n^1 - R_n^2)$. The stationary state, covering the entire system, is thus governed by the nucleation center with the smallest local threshold f_n^{min}.

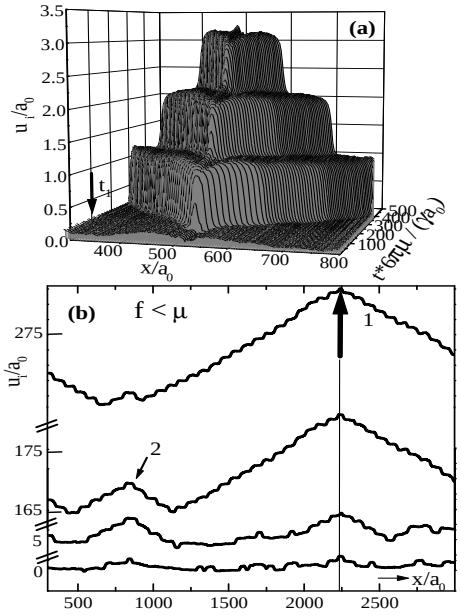

FIG. 2. Evolution of *longitudinal* displacements $u_i(t)$ plotted for clarity in a transverse way vs. x ($\Delta = 0.025$): (a) Nucleation of defect pairs in the commensurate chain of Fig. 1 ($L = 1000a_0$). (b) Transient response for a system with $L = 3000a_0$. The labels 1 and 2 mark competing nucleation centers in the long time dynamics.

Next, we turn to the *f-v* curves in Fig. 1 at incommensurability ($w/b_0 = 0.98$, small defect density $c_d \sim 1/2l_d$). In contrast to the curve for $\Delta = 0$ (full line), the data for $\Delta = 0.025$ show a significant threshold force due to pinning of the existing defects by random strains in the CE's. We define the pinning force for a single defect as $f_d(x)$ with a distribution $\{f_d\}$ along the channel and a maximum value f_d^{max}. The shape of the distribution is roughly gaussian and has a width $\sim 0.1\mu$. The threshold force for a single defect will be $f_c = f_d^{max}$. If the defect density is low, the defects occupy only the highest values of $\{f_d\}$ and $f_c \lesssim f_d^{max}$ which in Fig. 1 is $f_c \simeq 0.2\mu$. Once defects are depinned, their velocity v_d fluctuates spatially and $\langle v_d \rangle$ is smaller than v_d^0. However, these effects strongly decrease with velocity and for $f \gtrsim 2f_d^{max}$ one retains a low mobility regime with $dv/df \simeq c_d v_d^0 a_0$, as seen in Fig. 1. Considering the regime of larger drive, the data exhibits a velocity upturn for $f \sim f_n^{min}$. At this driving force *new* defect pairs start to nucleate at a strong disorder fluctuation with a rate that exceeds the one at which *existing* defects travel trough the system.

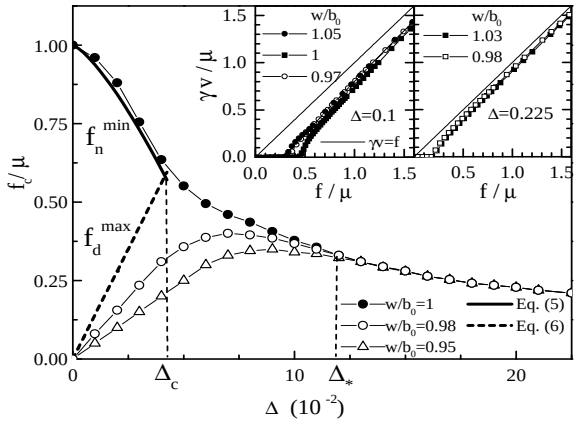

FIG. 3. Threshold force f_c, defined by a criterion $v_c \approx 0.02\mu/\gamma$, versus Δ for $w = b_0$ ($\bullet$), $w/b_0 = 0.98$ ($\circ$) and $w/b_0 = 0.95$ ($\triangle$). The thick solid and dashed lines represent Eqs. (5) and (6). The typical disorder strengths Δ_c and Δ_* are indicated. The insets show *f-v* curves for $\Delta > \Delta_c$.

Let us now discuss the disorder dependence of the threshold forces. Shown in Fig. 3 are f_c data versus Δ for commensurate and incommensurate chains. For $w = b_0$ the minimum from many disorder realizations is plotted, i.e. $f_c = f_n^{min}$. With growing disorder f_n^{min} decreases sharply while for the incommensurate chain with $w/b_0 = 0.98$, $f_c \sim f_d^{max}$ grows linearly. This behavior changes at $\Delta \simeq \Delta_c$ where Δ_c is defined as the disorder strength where for $w = b_0$ defects first appear spontaneously. Above Δ_c both curves (in)decrease more slowly with disorder and eventually merge. This change in behavior is due to the fact that favorable nucleation sites in the commensurate case act as strong pinning site for defects in the incommensurate case. The simulations show that the presence of pinned defects strongly affects the formation of a new nucleus. As a result, f_n^{min} decreases more slowly at larger disorder, i.e. at a higher density of pinned defects. The curve for $w/b_0 = 0.95$, for which the density of static, mismatch induced defects is $c_d \simeq l_d^{-1}$, shows a reduced threshold force and merges with the other curves at a disorder strength $\Delta = \Delta_*$. For $\Delta > \Delta_*$, disorder induced defects start to overlap (i.e. their density becomes $\gtrsim l_d^{-1}$) and f_c decreases further. The large disorder also has a pronounced effect on the shape of the *f-v* curves. As shown in the insets to Fig. 3, the typical low mobility regime at weak mismatch has vanished and all curves exhibit linear behavior, except in a small regime for f just above f_c.

To uncover the underlying physics of the phenomena described above, we now propose an analytical description of our system. The energy of a vortex in the channel at $\mathbf{r_0} = (x, 0)$ due to interaction with shifted vortices in the CE's is:

$$V(\mathbf{r_0}) = (2\pi)^{-2} \int d\mathbf{k} V(\mathbf{k}) \rho_e(\mathbf{k}) e^{i\mathbf{k}\cdot\mathbf{r_0}}. \qquad (2)$$

$V(\mathbf{k}) = 2\pi U_0/(\mathbf{k}^2 + \lambda^{-2})$ with $U_0 = \Phi_0^2/2\pi\mu_0\lambda^2$, and $\rho_e(\mathbf{k})$ are the Fourier transforms of the London potential and the vortex density in the edge, respectively. For weak disorder ($\nabla \cdot \mathbf{d} \ll 1$), ρ_e can be decomposed [11]: $\rho_e(\mathbf{r}_e, \mathbf{d}) \simeq (B/\Phi_0)(1 - \nabla \cdot \mathbf{d} + \delta\rho_e)$ where $\delta\rho_e = \sum_i \cos[\mathbf{K}_i(\mathbf{r}_e - \mathbf{d}(\mathbf{r}_e))]$ and $\mathbf{K}_i$ spans the reciprocal lattice. Substitution in Eq. (2) yields two terms: a quasi-periodic potential $V^p \simeq (\mu/k_0)\sin[k_0(x - d)]$, with $k_0 = 2\pi/a_0$ [12] due to $\delta\rho_e$ of the vortex rows nearest to the CE's, and a random, nonlocal contribution coming from the density fluctuations: $V^r(\mathbf{r_0}) = -(B/\Phi_0)\int d\mathbf{r}_e V(\mathbf{r_0} - \mathbf{r}_e)\nabla \cdot \mathbf{d}(\mathbf{r}_e)$ with correlator:

$$\langle V^r(0)V^r(x)\rangle \simeq 4\Delta^2 U_0^2 (\lambda/a_0)^{1+\alpha} e^{-(x/\lambda)^2}. \qquad (3)$$

Here α depends on the disorder correlations between the rows m in the CE's. We choose $\partial_x d(x)$ to be independent of row number, which yields $\alpha = 2$.

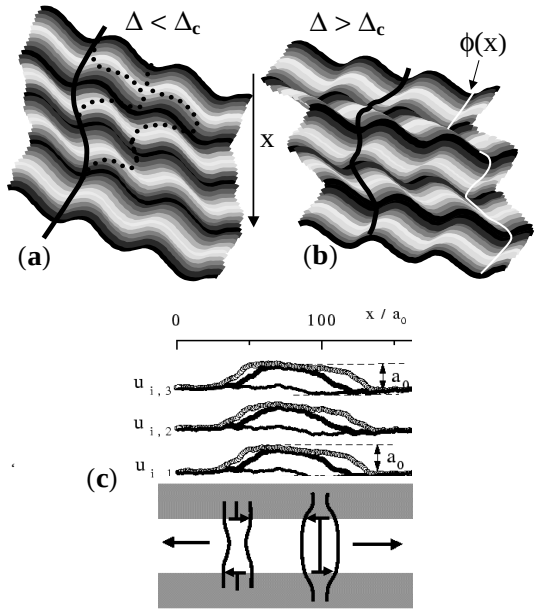

FIG. 4. (a,b) Mechanical representation of Eq. (4). (a) For $\Delta < \Delta_c$ a gap exists between the barrier for defect nucleation (dashed) and defect pinning. (b) When $\Delta > \Delta_c$ disorder induced defects are always present below f_c. The white line shows the random phase $\phi(x)$ of the washboard potential. (c)top: Evolution of longitudinal displacements of individual rows at depinning for $w/b_0 = 3$ and $\Delta = 0.02$. (c)bottom: Square lattice representation of the nucleated stacks of discommensurations. Small arrows indicate the Burgers vector of the dislocations terminating each stack.

To obtain a continuum description of the chain in terms of the displacement field $u(x)$, the vortex density ρ_c *in* the channel is decomposed, as was done for ρ_e. The resulting interaction of the chain with the CE's is $H_p = a_0^{-1}\int (V^p + V^r)[\delta\rho_c(x, u) - \partial_x u]dx$. For $\lambda > a_0$, both V^r and $\partial_x u$ vary slowly while V^p and $\delta\rho_c$ oscillate rapidly and only two terms in H_p remain [13]. The

force $-\delta H_p/\delta u$ on the chain thus contains a commensurate term and a random compression term $-\partial_x V^r(x)$, which is independent of u. We obtain the equation of motion for u by adding the *intra-chain* force $\kappa\partial_x^2 u$, with stiffness $\kappa \simeq U_0\pi(\lambda/a_0)$ [14], resulting in:

$$\gamma\partial_t u = f + \kappa\partial_x^2 u - \mu\cos(k_0 u) - \partial_x V^r(x). \qquad (4)$$

The reduced stiffness is now $g = \kappa/(k_0\mu a_0^2) = 3\pi(\lambda/a_0)$. Eq. (4) describes the transverse displacements of an elastic string in a tilted washboard potential with random phase $\phi(x) = -\int_{-\infty}^{x} dx' V^r(x')/\kappa$, see Fig. 4. It corresponds to a commensurate CDW with random forward scattering [15] rather than the usual model for a CDW in which the commensurability potential is ignored either due to strong *direct* random coupling to u or due to large mismatch [16].

Next, the dependence of f_n^{min} and f_d^{max} on the strain Δ can be addressed by considering a deformation in the CE's of wavelength l_{dis}: $\partial_x d(\mathbf{r}) = \Delta\sin(2\pi x/l_{dis})$. When $l_{dis} \gg \lambda$, the last term in Eq. (4) simplifies to $-\partial_x V^r \simeq g^2\Delta U_0/(2\sqrt{3}l_{dis})\cos(2\pi x/l_{dis})$. To describe nucleation (for $f \gtrsim \mu/2$), we need the string displacements $\delta(x) = u - u_0$ relative to the minimum of the *tilted* washboard potential given by $u_0 = -k_0^{-1}[2(1-f/\mu)]^{1/2}$. The restoring force for such displacements is $\mu k_0^2 u_0\delta(x)$, while the elastic force is $\kappa\partial_x^2\delta$. Balancing these with $\partial_x V^r$ yields $\delta(x) = \delta_0\cos(2\pi x/l_{dis})$. The amplitude of the displacement $\delta_0 \sim l_{dis}/(l_d^2 + k_0|u_0|l_{dis}^2)$ is largest for a wavelength $l_{dis} = l_d/\sqrt{k_0|u_0|}$ resulting in $\delta_0^{max} \simeq \sqrt{3}a_0 g^{3/2}\Delta/(8\pi\sqrt{k_0|u_0|})$. Since the *critical* displacement at which the string depins is $\simeq |u_0|$ [8], the minimum nucleation force follows from $|u_0| = \delta_0^{max}$:

$$f_n^{min}/\mu \simeq 1 - \left[4\Delta g^{3/2}/(5\sqrt{3})\right]^{4/3}. \qquad (5)$$

For an *existing* defect at zero drive, the pinning energy is $E_{d,p}(x) = a_0^{-1}\int dx'\partial_x u_d(x'-x)V^r(x')$ with u_d the familiar shape of a sine-Gordon kink [8] centered at x and of size l_d. Optimal pinning occurs for deformations in the CE's with $l_{dis} = l_d$, similar to the 'optimal' size of a nucleation center for $f \simeq \mu/2$. The maximum defect pinning force is then given by:

$$f_d^{max}/\mu \simeq \Delta g^{3/2}/\sqrt{3}. \qquad (6)$$

The results (5) and (6) are plotted in Fig. 3, using $g = 9$ as in the simulations. Eq. (5) agrees with the numerical data, while Eq. (6) can be considered as upper bound. The curves merge at $\Delta_c \simeq \sqrt{3}g^{-3/2}/2$, where pinned defects can appear spontaneously in the channel [17].

The disorder strength Δ_* where the density of disorder induced defects becomes $\sim l_d^{-1}$ can be estimated by equating the typical (rms) pin energy of a defect with its bare energy $\sim \mu a_0\sqrt{g}$. The former is estimated using the previous form for $E_{d,p}$ and Eq. (3): $\langle(E_{d,p})^2\rangle^{1/2} \simeq 2U_0(g/3\pi)^{(2+\alpha)/2}g^{-1/4}\Delta$ leading to

$$\Delta_* \simeq (3\pi/4)g^{-5/4}, \qquad (7)$$

also in reasonable agreement with the data in Fig. 3. These results show that the effect of disorder rapidly grows on increasing the interaction range λ/a_0.

Finally, we shortly discuss how these results carry over to channels with *multiple* chains near matching ($w/b_0 \simeq n$, with n an integer ≥ 2). Without disorder f_c has sharp peaks at matching of height $f_c^0 = \mu b_0/w = \mu/n$ [4]. With disorder, the behavior of f_c is similar to that in Fig. 3 [18]. In Fig. 4(c) we show the depinning process for $w/b_0 = 3$, $\Delta = 0.02$ and $f = 0.7 f_c^0$. As observed, the defects involved with depinning consist of stacks of discommensurations, coupled between the chains. Each stack is terminated by a pair of dislocations with opposite Burgers vector *along* the CE's. This quasi-1D behavior at weak disorder can also be described by Eq. 4 by substituting μ/n for μ. For larger disorder the threshold near matching reduces to $\sim 30\%$ of f_c^0. The merging of the commensurate and weakly incommensurate threshold forces now occurs for $\Delta_*^n = \Delta_*/n^{1/4}$. For a realistic value of $\lambda/a_0 \sim 4$, we estimate $\Delta_* \sim 0.03$ meaning that rms strains in the CE's $\lesssim 2\%$ already cause strong disorder. At strong disorder *and large mismatch* the quasi-2D nature of the system causes new phenomena: for $w/b_0 \simeq n \pm 1/2$ transitions from $n \to n \pm 1$ rows occur, involving pinning of dislocations with *misaligned* Burgers vector [19]. The threshold force then *exceeds* f_c near matching [19].

In summary, depinning of a vortex chain in a channel formed by disordered vortex arrays with (nearly) the same periodicity, occurs by nucleation of defect pairs or motion of existing defects. The gap between the barriers for these two processes and the sharp peak in f_c at commensurability vanish with increasing disorder. For large disorder in the channel edges f_c saturates at a small fraction of the ideal lattice strength.

This project is supported by the Nederlandse Stichting voor Fundamenteel Onderzoek der Materie (FOM) and also by U.S.DOE, Office of Science under contract #W-31-109-ENG-38 during R.B.s stay at Argonne. V.M.V. is supported by U.S.DOE, Office of Science under contract #W-31-109-ENG-38.

[1] A.E. Koshelev and V.M. Vinokur, Phys. Rev. Lett. **73**, 3580 (1994); T. Giamarchi and P. Le Doussal, *ibid.*, **76**, 3408 (1996); L. Balents and M.P.A. Fisher, *ibid.* 75, 4270 (1995); G. Blatter *et al.*, Rev. Mod. Phys. **66**, 1125, (1994).

[2] H.J. Jensen *et al.*, Phys. Rev. Lett. **60**, 1676 (1988).

[3] A. Pruymboom *et al.*, Phys. Rev. Lett. **60**, 1430 (1988); M.H. Theunissen *et al.*, *ibid.*, **77**, 159 (1996).
[4] R. Besseling *et al.*, Phys. Rev. Lett. **82**, 3144 (1999).
[5] J. Krug, Phys. Rev. Lett. **75**, 1795 (1995).
[6] B.A. Malomed, Phys. Rev. B **39**, 8018 (1989).
[7] In the experiment, d^y is assumed to be suppressed due to screening currents along the channel edges. See also B.L.T. Plourde *et al.*, Phys. Rev. B **66**, 054529 (2002).
[8] M. Büttiker and R. Landauer, Phys. Rev. A. **23**, 1397 (1981).
[9] Representative movies are available at http://lions1.leidenuniv.nl/wwwhome/rbessel.
[10] C.R. Myers and J.P. Sethna, Phys. Rev. B **47**, 11171 (1993); D. Cule and T. Hwa, Phys. Rev. Lett. **77**, 278 (1996).
[11] T. Giamarchi and P. Le Doussal, Phys. Rev. B **52**, 1242 (1995).
[12] We obtain $\mu = U_0/6\pi a_0 \equiv 2a_0\tau^0$ with $\tau^0 = a_0 c_{66}/(2\pi b_0)$ as expected for a harmonic potential between rows spaced by b_0 with intra-row spacing a_0, J. Frenkel, Z. Phys. **37**, 572 (1926).
[13] The product $V^p\rho_c$ in fact yields $(\mu/k_0)\sin[k_0(u-d)]$. The resulting extra random phase $-k_0 d$ in the cos term in (4) is ignored since it is small compared to the phase ϕ arising from V^r.
[14] The full, dispersive expression for the stiffness is $\kappa(k) = U_0\pi(\lambda/a_0)/\sqrt{1+\lambda^2k^2}$. Thus Eq. (4) applies for $k < \lambda^{-1}$.
[15] M.V. Feigelman and V.M. Vinokur, Solid State Communications, **45**, 595 (1983); V.M. Vinokur and M.B. Mineev, Zh. Eksp. Teor. Fiz. **88** 1809 (1985).
[16] H. Fukuyama and P.A. Lee, Phys. Rev. B **17**, 535 (1978); P.B. Littlewood, *ibid.* **33**, 6694 (1986).
[17] Since, for depinning, the 'optimal' wavelengths are at least l_d, the results are valid when $l_d > 2\pi\lambda$. Using $l_d = 2\pi a_0\sqrt{g}$, this corresponds to the range $\lambda/a_0 \lesssim 10$.
[18] R. Besseling, Ph. D. Thesis, Leiden University (2001); R. Besseling *et al.*, to be published.
[19] N. Kokubo *et al.*, Phys. Rev. Lett. **88**, 247004 (2002).